Microsc. Microanal. 17, 215–219, 2011
doi:10.1017/S1431927610094201

Microscopy AND Microanalysis

High-Resolution Imaging of Kidney Vascular Corrosion Casts with Nano-CT

Roger Wagner,[1,*] Denis Van Loo,[2,3] Fred Hossler,[4] Kirk Czymmek,[1] Elin Pauwels,[2] and Luc Van Hoorebeke[2]

[1]*Department of Biological Sciences, University of Delaware, Newark, Delaware 19716, USA*
[2]*UGCT, Department of Physics and Astronomy, Ghent University, Ghent, Belgium*
[3]*Department of Soil Management and Soil Care, Ghent University, Ghent, Belgium*
[4]*Department of Anatomy and Cell Biology, Quillen College of Medicine, East Tennessee State University, Johnson City, Tennessee, USA*

Abstract: A vascular corrosion cast of an entire mouse kidney was scanned with a modular multiresolution X-ray nanotomography system. Using an isotropic voxel pitch of 0.5 μm, capillary systems such as the vasa recta, peritubular capillaries and glomeruli were clearly resolved. This represents a considerable improvement over corrosion casts scanned with microcomputed tomography systems. The resolving power of this system was clearly demonstrated by the unique observation of a dense, subcapsular mat of capillaries enveloping the entire outer surface of the cortical region. Resolution of glomerular capillaries was comparable to similar models derived from laser scanning confocal microscopy. The high-resolution, large field of view and the three-dimensional nature of the resulting data opens new possibilities for the use of corrosion casting in research.

Key words: nano-CT, X-ray tomography, corrosion casts, computer modeling

Introduction

Microscopy of vascular corrosion casts has greatly improved our understanding of the three-dimensional (3D) geometry of blood vascular systems (Djoniv & Burris, 2004, review). Sharp, high-resolution images of corrosion casts can be viewed with the scanning electron microscopy (SEM), but the angle of viewing is limited and internal cast detail is often hidden. A solution to these limitations is the optical sectioning of corrosion casts using confocal microscopy and modeling of the 3D data. These models can be viewed from any angle and internal regions can be imaged (Kaczmarek & Becker, 1997; Wagner et al., 2006; Wagner & Hossler, 2008). However, the field-of-view of a confocal microscope is relatively limited, and only small regions of casted vascular systems can be imaged when using an oil immersion objective lens required for 3D fidelity. This limitation has been overcome by utilizing X-ray tomography. Casting polymers exhibit sufficient X-ray density to obtain tomographic datasets representing entire organs. The resolution afforded by Micro-CT systems, however, limits viewing large casted vessels, while microvessels and capillaries remain unresolved (Wagner & Hossler, 2008). Nano-CT systems provide a true resolution of 1 μm and less. We present here Nano-CT modeling of a corrosion-casted mouse kidney. The sample is ideal because of its rich supply of capillaries and specialized vascular structures (glomeruli). Casts of vessels of all calibers are clearly imaged, and the resolution closely approximates that provided by confocal microscopy with a greatly enhanced field of view.

Received July 16, 2010; accepted September 29, 2010
*Corresponding author. E-mail: Rags@udel.edu

Materials and Methods

Preparation of Corrosion Casts of Mouse Kidney

Mice (C57BL/6 NHsd from Harlan Laboratories, Indianapolis, IN, USA) were sacrificed (IACUC approved protocol) by CO_2 narcosis and pinned onto a paraffin surface in preparation for dissection. In some cases mice were anticoagulated by an intra-abdominal injection of 0.5 mL sodium heparin (1,000 U/mL) 10 min before narcosis. The thorax was opened, and the thoracic aorta exposed. A glass cannula was attached to polyethylene tubing and a 10cc syringe barrel. Both were held in place by a micromanipulator and the cannula was inserted into the aorta in an anterior to posterior direction and secured into place with a ligature placed around the cannulated section of the vessel.

Prior to insertion of the cannula, the syringe barrel was filled with 37°C physiological saline, and the tubing and cannula were flushed of air with the warm saline. The cannulating apparatus was prepared prior to the procedure by heating a piece of 100 μL glass sampling pipette tubing over a flame, drawing it out to a diameter about equivalent to the diameter of the vessel to be cannulated, and then inserting its opposite end into a section of polyethylene tubing (PE 250). The tubing was inserted into a 15 gauge Luer stub adapter attached to the 10cc syringe barrel. A $\frac{1}{16}$ in. T-connector with a side arm of polyethylene tubing was attached along the main tubing to allow for release of any air bubbles that might be present in the tubing prior to injection. A clamp was attached to the side arm tubing so it could be opened and closed as needed to release air. Once the aortic cannula was tied into place, the vena cava was opened to allow blood drainage. The vasculature below the

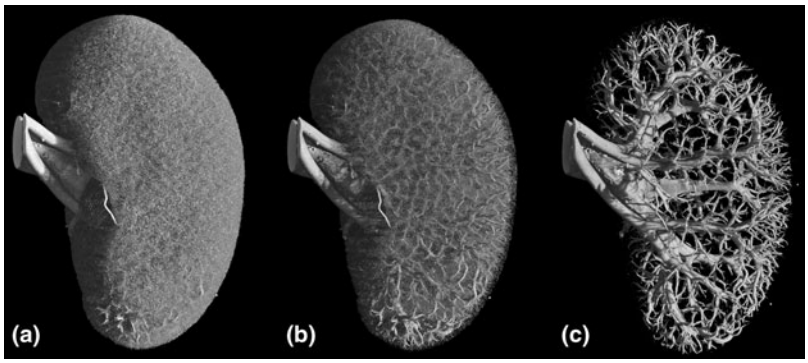

Figure 1. a: Reconstructed scan of an entire mouse kidney corrosion cast. A finely-textured layer of capillaries was seen lining the entire cortical surface of the kidney. These were densely packed and probably lie just beneath the connective tissue capsule of the kidney. Res. 7.5 μm voxel pitch. **b,c:** Gradual elimination of the smaller vessels from the model by thresholding revealed the larger vessels that comprised the vascular tree of the entire kidney. Res. 7.5 μm voxel pitch.

diaphragm was then flushed of blood with the warm saline by light manual pressure on the syringe barrel or by compressing the syringe barrel with a hand operated screw. Usually about 10cc of saline was flushed through the vasculature. A 10cc syringe containing Mercox casting resin then replaced the saline syringe.

The resin (Ladd Research Industries, Williston, VT, USA) was prepared just prior to use by combining 4cc of Mercox with 1cc methyl methacrylate (Sigma-Aldrich Co., St. Louis, MO, USA) and 0.15cc catalyst (benzoyl peroxide). The polyethylene tubing was flushed of any air bubbles using the T-connector side arm on the tubing prior to infusing the resin into the vasculature. The resin was pushed into the vasculature by light pressure on the syringe barrel as before until all of it was inserted or until polymerization occurred. Excess resin was seen extruding from the open end of the vena cava prior to completion of the injection. Initial polymerization of the resin usually required about 10 min, but the intact mouse carcass was placed in a 60°C water bath for 30 min following the procedure to insure complete polymerization of the resin. After detaching the cannulating apparatus, the carcass was placed in 5% KOH in a 60°C oven overnight and then gently rinsed in water for several hours to remove dissolved tissue. The KOH treatment and water rinse were repeated until all the tissue was dissolved (usually four times). Casts were cleaned by immersion in 5% formic acid for 15 min, rinsed thoroughly in distilled water, frozen in distilled water, and lyophilized (Lametschwandtner et al., 1990). Lyophilization reduced the collapse of fine capillary beds, which may result from surface tension encountered with air drying.

Acquisition of CT Scans

The corrosion casted samples were scanned using a modular multiresolution X-ray tomography system developed at the Ghent University Centre for X-ray tomography (www.ugct.ugent.be). The system consists of eight motorized stages, two X-ray detectors, and two X-ray tubes, which deliver optimal image resolution and quality for samples up to 37 cm in diameter. The raw data obtained were processed and reconstructed with an in-house developed software package—"Octopus" (Vlassenbroeck et al., 2007).

The entire corrosion cast of the mouse kidney was scanned using an amorphous silicium panel detector (Varian Paxscan 2520) with a CsI scintillator and 127 μm pixel pitch in combination with a directional target X-ray tube operated at 70 kV. The sample was rotated 360° in steps of 0.3° and X-ray projections of 3.6 s exposure time collected at every angle. This resulted in 1,200 projection images of 1820×1450 pixels after approximately 1 h of scanning. The final voxel pitch after reconstruction is 7.5 μm. Subsequently a subvolume scan of the kidney was performed with similar settings at a voxel pitch of 4.2 μm. A small part of the cast was dissected, and similar scans were performed with the same set of components and parameters but with 1,000 projections of 4.2 s, resulting in scans of 1.4 and 0.77 μm voxel pitch for the entire dissected part and subvolume scan. A casted glomerulus was extracted and scanned separately with a transmission target X-ray tube and a charge-coupled device camera with a gadox scintillator (Photonic Science VHR) and 7.7 μm pixel pitch. The detector was used with 8×8 binning and 400 projections taking 3.5 s per projection. Projections were recorded at an angle interval of 0.9° resulting in a scan with 0.5 μm voxel pitch.

Results

Reconstructed scans of entire mouse kidney corrosion casts at 7.5 μm voxel pitch revealed a finely textured layer of capillaries lining the entire outer surface of the cortical region (Fig. 1a). The dense packing of this capillary mat (Fig. 2) suggested that it lay beneath the connective tissue capsule of the kidney rather than within the capsule. Subtraction of microvessels from the reconstruction by gray-scale thresholding revealed the vascular tree of larger vessels throughout the entire kidney (Fig. 1b,c). Since partial volume effects reduce the local density in regions where smaller structures are present, by increasing the lower threshold, larger vessels become apparent. Saggital bisection (Fig. 3) and projection (Fig. 4) images of whole kidney reconstructions showed renal arteries and veins at the pelvis and arcurate and intralobular arteries and veins. In the medullary region, capillaries of the vasa recta were closely packed and radiated toward the cortex. Orthoslices in x, y, and z planes (Fig. 5) revealed distinct medullary and cortical regions with arcurate arteries and veins demarcating the boundary between them.

Dissected regions of the cortex at 1.3 μm voxel pitch revealed glomerular and peritubular capillaries (Fig. 6). At

Figure 2. The subcortical capillary mat was resolved into individual vessels with minimal interstitial spaces between them. Res. 7.5 μm voxel pitch.

Figure 3. A saggital bisection of the kidney exhibits renal arteries, veins, and interlobular arteries. Filament-like capillaries of the vasa recta radiate from the kidney hilus toward the cortex. Res. 7.5 μm voxel pitch.

0.77 μm voxel pitch (Fig. 7), these peritubular capillaries surrounded empty space normally occupied by proximal and distal tubules appeared irregular in shape and nearly sinusoidal. A single extracted glomerulus scanned with a 0.5 μm voxel pitch (Fig. 8) revealed a branched network of casted capillaries clearly resolved and with a resolution comparable to a similar model obtained with confocal microscopy (Fig. 9).

Discussion

Corrosion casts provide an accurate representation of the 3D geometry of vascular systems. Various methods have been used to acquire 3D datasets from casts. Since some casting polymers exhibit fluorescent properties, the confocal laser scanning microscope can acquire fluorescent optical sections through corrosion casts. The voxelated 3D datasets obtained in this way can be used to create a model, which can be viewed from any angle and valuable quantitative data such as surface area; volume and length of casted vessels can be calculated (Castenholz, 1995; Kaczmarek & Becker, 1997; Rodriguez-Baeza et al., 1998; Czymmek et al., 2001; Wagner et al., 2005, 2006). Confocal microscopy can adequately resolve the smallest capillaries within a cast such as those in the glomerulus of the kidney (Wagner et al., 2006). However, due to the limited field of view of the confocal microscope especially for high-magnification objectives, only small regions of casted vascular systems can be visualized.

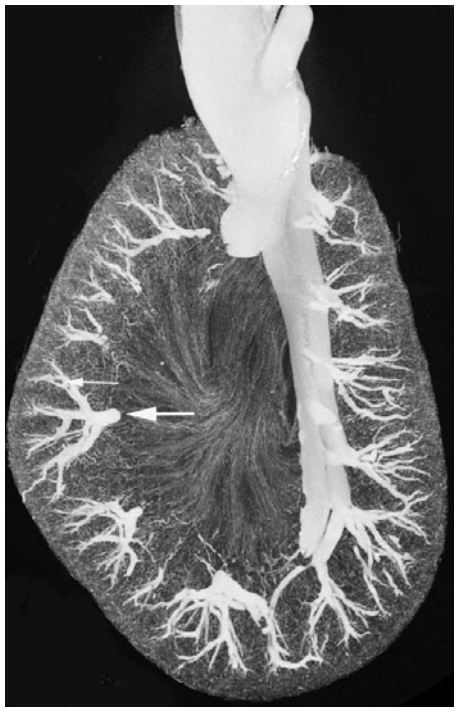

Figure 4. Projection image of a thick slice through the kidney model. Capillaries of the vasa recta were clearly resolved in the medullary region. Interlobular (large arrow) and intralobular (small arrow) arteries and veins projected into the cortex. Res. 7.5 μm voxel pitch.

To acquire larger volumes of 3D data from corrosion casts, tomographic X-ray scanning of casts with Micro-CT has been employed (Bentley et al., 2002; Sled et al., 2004; Marxen et al., 2004; Rennie et al., 2007; Muller et al., 2008; Wagner & Hossler, 2008; Mondy et al., 2009; Folarin et al., 2010). However, due to limited resolution of the Micro-CT systems, the true submicron resolution of Nano-CT systems is preferred for detailed studies of the smallest capillary structures.

By utilizing the modular multiresolution X-ray tomography system developed at the Ghent University Centre for X-Ray Tomography, we have been able to visualize the smallest capillaries in a kidney corrosion cast down to a

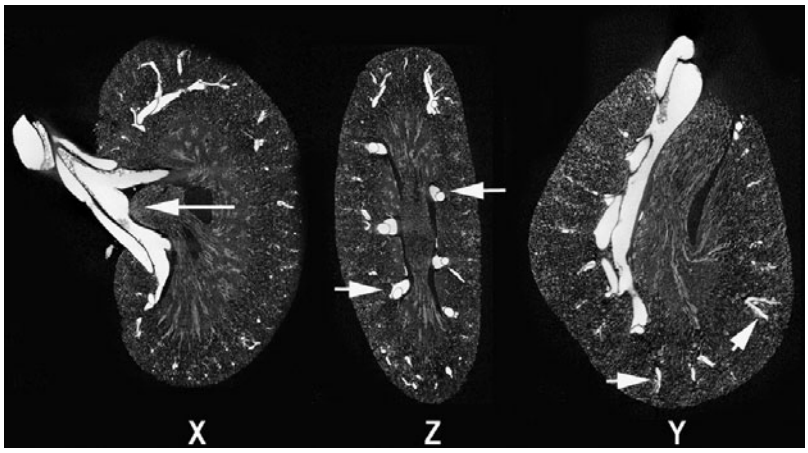

Figure 5. Orthoslices through *x*, *y*, and *z* planes of the kidney model. The cortical and medullary regions were clearly demarcated, and the area cribosa of the single pyramid of rodents was evident (*x* plane-arrow). Arcurate arteries and veins were seen at the boundary between the cortex and the medulla (*z* plane-arrow). Portions of interlobular arteries were observed in the *y* plane (arrow). Res. 7.5 μm pixel pitch.

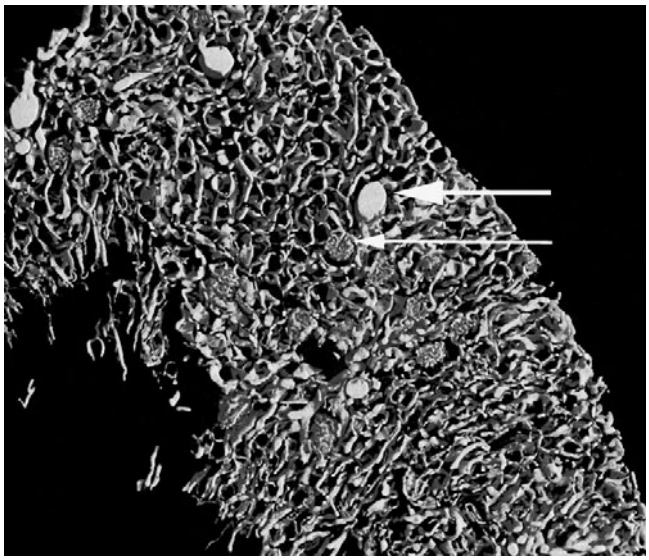

Figure 6. Dissected region of the cortex showed intralobular vessels (large arrow), glomeruli (small arrow), and numerous peritubular capillaries. Res. 1.3 μm voxel pitch.

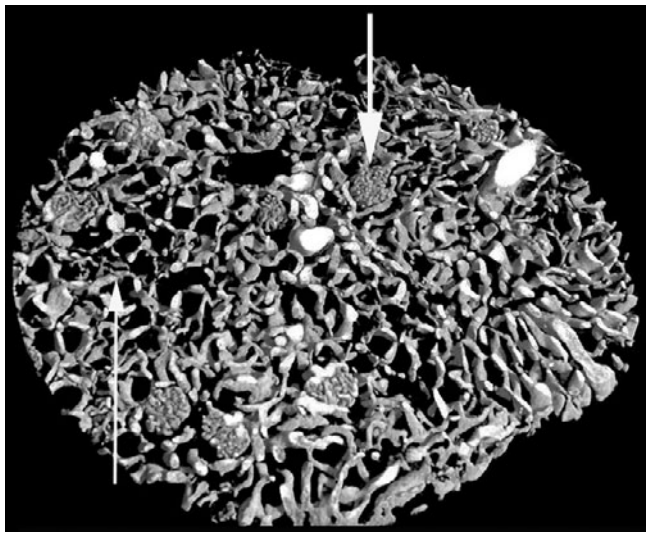

Figure 7. Cylindrical sample of a dissected portion of the cortex. Capillaries of the glomeruli were resolved (large arrow) as well as peritubular capillaries (small arrow), which were irregular in shape and surrounded spaces normally occupied by proximal and distal tubules. Res. 0.77 μm voxel pitch.

resolution of 0.5 μm voxel pitch. This Nano-CT system is capable of acquiring datasets from an entire mouse kidney in which larger vessels of the vascular tree can be seen as well as the smallest diameter capillaries such as those of the vasa recta, glomerular capillaries, and peritubular capillaries.

The power of this technology is amply demonstrated in the revealing of a subcapsular mat of capillaries surrounding the entire kidney surface. This would have remained undetected using a lower resolution Micro-CT system. A smaller visual field such as that of a confocal microscope would not have revealed the extensiveness of this capillary plexus. It is possible that this rich capillary bed may account for the fact that subcapsular transplantation of ectopic tissues in the kidney has been so successful (Robertson et al., 2007).

Nano-CT of corrosion casts makes it possible to model the entire circulatory geometry of entire organs down to the capillary level. This will improve our understanding of blood circulation in normal tissues and organs and also

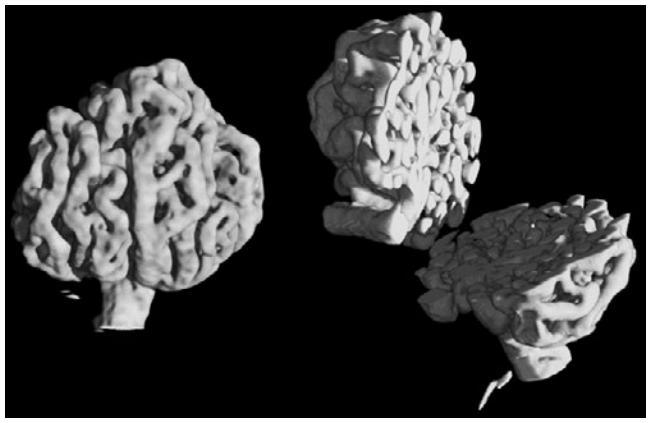

Figure 8. A single extracted glomerulus. Branched capillaries were clearly resolved. The model was also sliced to view the interior of the glomerulus. Res. 0.5 μm voxel pitch.

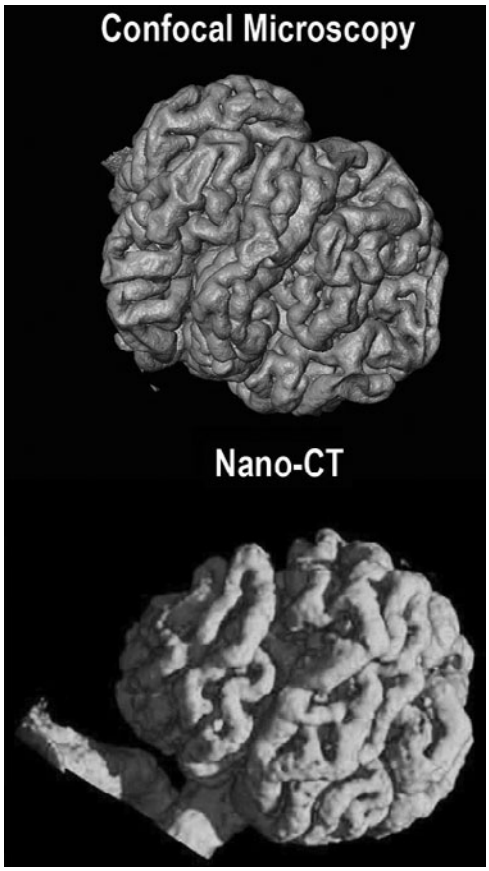

Figure 9. At 0.5 μm voxel pitch the Nano-CT scan of a glomerulus exhibited a resolution comparable to a similar model generated with the confocal microscope also at 0.5 μm voxel pitch.

in abnormal disease conditions such as tumors and hemangiomas.

Acknowledgments

The Fund for Scientific Research–Flanders (FWO) is acknowledged for the doctoral grant to D. Van Loo (G.0100.08), and the special research fund of Ghent University is acknowledged for their financial support (CRA.01G01008).

References

Bentley, M.D., Ortiz, M.C., Ritman, E.L. & Carlos-Romero, J. (2002). The use of microcomputed tomography to study microvasculature in small rodents. *Am J Physiol Reg Integrative Comp Physiol* **282**, 1267–1279.

Castenholz, A. (1995). Examination of injected specimens by confocal laser scanning microscopy and scanning electron microscopy. *Scanning Microscopy* **9**, 1245–1254.

Czymmek, K., Wagner, R., Hossler, F. & Kao, R. (2001). Imaging and volumetric quantitation of vascular corrosion casts with laser scanning confocal microscopy. *Microsc Microanal* **6**(S2), 562–563 (CD-ROM).

Djoniv, V. & Burris, P. (2004). Corrosion cast analysis of blood vessels. In *Methods in Endothelial Cell Biology*, Augustin, H.G. (Ed.), Chap. 3, pp. 47–60, Berlin, Heidlburg: Springer-Verlag.

Folarin, A.A., Konerding, M.A., Timonen, J., Nagl, S. & Pedley, R.B. (2010). Three-dimensional analysis of tumour vascular corrosion casts using stereoimaging and micro-computed tomography. *Microvasc Res* **80**, 89–98.

Kaczmarek, E. & Becker, R. (1997). Three dimensional modeling of renal glomerular capillary networks. *Anal Quant Cytol Histol* **19**, 93–101.

Lametschwandtner, A., Lametschwandtner, U. & Weiger, T. (1990). Scanning electron microscopy of vascular corrosion casts, techniques and applications: An updated review. *Scanning Microscopy* **4**, 889–941.

Marxen, M., Thornton, M., Chiarot, C., Klement, G., Kopruinikar, J., Sled, J. & Henkleman, R. (2004). Micro-CT scanner performance and considerations for vascular imaging. *Med Phys* **31**(2), 305–313.

Mondy, W., Cameron, D., Timmermans, J., DeClereck, N., Sasov, A., Casteleyn, C. & Piegl, L. (2009). Micro-CT of corrosion casts for use in the computer-aided design of microvasculature. *Tissue Eng* **15**, 1–10.

Muller, B., Lang, S., Dominietto, M., Rudin, M., Schulz, G., Dehyle, H., Germann, M., Pfieffer, F., David, C. & Weitkamp, T. (2008). High resolution tomographic imaging of microvessels. *Proceedings SPIE. Developments in X-Ray Tomography*, Stock, S.R. (Ed.), vol. 7078, pp. 1–10.

Rennie, B., Whitely, K., Kulandevelu, S., Adamson, S. & Sled, J. (2007). 3D visualization and quantification by microcomputed tomography of late gestational changes in the arterial and venous feto-placental vasculature of the mouse. *Placenta* **28**(8), 833–840.

Robertson, N., Faichild, P. & Waldeman, H. (2007). Ectopic transplantation under the kidney capsule. *Meth Molec Biol* **380**, 347–353.

Rodriguez-Baeza, A., Reina-Dela Torre, F., Ortega-Sanchez, M. & Sahuguillo-Barris, J. (1998). Perivascular structures in corrosion casts of the central nervous system: A confocal laser and scanning electron microscope study. *Anat Rec* **252**, 176–184.

Sled, J., Marxen, M. & Henkelman, R. (2004). Analysis of microvasculature in whole kidney specimens using micro-ct. *Proceedings of SPIE. Developments in X-Ray Tomography*, Bonse, U. (Ed.), vol. 5535, pp. 53–64.

Vlassenbroeck, J., Dierick, M., Massachaele, B., Cnudde, V., Van Hoorebeke, L. & Jacobs, P. (2007). Software tools for quantification of X-ray microtomography at the UGCT. *Nucl Instrum Meth Phys Res A* **580**(1), 442–445.

Wagner, R., Czymmek, K. & Hossler, F. (2005). Confocal microscopy, modeling and quantitation of corroded and noncorroded casts of microvascular systems. *Microsc Microanal* **11**(S2), 1208–1209 (CD-ROM).

Wagner, R., Czymmek, K. & Hossler, F. (2006). Confocal microscopy, computer modeling and quantification of glomerular vascular corrosion casts. *Microsc Microanal* **12**, 262–268.

Wagner, R. & Hossler, F. (2008). Tomographic modeling of casted vascular systems. *Infocus; Proc Royal Microscopal Society* **11**, 4–21.